Lotus japonicus symbiosis signaling genes and their role in the establishment of root-associated bacterial and fungal communities

Rafal Zgadzaj[§ 1,2], Thorsten Thiergart[§ 1], Zoltán Bozsóki [3], Ruben Garrido-Oter [1,2], Simona Radutoiu[*3], and Paul Schulze-Lefert[*1,2]

[1]Max Planck Institute for Plant Breeding Research, 50829 Cologne, Germany.

[2]Cluster of Excellence on Plant Sciences (CEPLAS), Max Planck Institute for Plant Breeding Research, 50829 Cologne, Germany.

[3]Department of Molecular Biology and Genetics, Faculty of Science and Technology, Aarhus University, 8000 C Aarhus, Denmark.

§ joint first authors

* co-corresponding authors, (radutoiu@mbg.au.dk , S.R., schlef@mpipz.mpg.de , P.S.-L.)

Abstract

The wild legume *Lotus japonicus* engages in mutualistic symbiotic relationships with arbuscular mycorrhiza (AM) fungi and nitrogen-fixing rhizobia. Using plants grown in natural soil and community profiling of bacterial 16S *rRNA* genes and fungal internal transcribed spacers (ITS), we examined here the role of the *Lotus* symbiosis genes *RAM1*, *NFR5*, *SYMRK*, and *CCaMK* in structuring bacterial and fungal root-associated communities. We found host genotype-dependent community shifts in the root and rhizosphere compartments that were mainly confined to bacteria in *nfr5* or fungi in *ram1* mutants, whilst *symRK* and *ccamk* plants displayed major changes across both microbial kingdoms. We observed in all AM mutant roots an almost complete depletion of a large number of Glomeromycota taxa that was accompanied by a concomitant enrichment of Helotiales and *Nectriaceae* fungi, suggesting compensatory niche replacement within the fungal community. A subset of Glomeromycota whose colonization is strictly dependent on the common symbiosis pathway was retained in *ram1* mutants, indicating that *RAM1* is dispensable for intraradical colonization by some Glomeromycoyta fungi. However, intraradical colonization by certain Burkholderiaceae taxa is dependent on AM root infection, thereby revealing a microbial interkingdom interaction. Our findings imply a broad role for *Lotus* symbiosis genes in structuring the root microbiota.

Introduction

Mutualistic plant-microbe interactions are essential adaptive responses dating back to plant colonization of terrestrial habitats [1,2]. Endosymbiotic association with obligate arbuscular mycorrhizal (AM) fungi belonging to the phylum Glomeromycota is considered to have enabled early land plants to adapt to and survive harsh edaphic conditions by improving the acquisition of nutrients, especially phosphorus, and water from soil [3]. It is estimated that approximately 80% of extant plant species remain proficient in AM symbiosis (AMS), testifying to its importance for survival in natural ecosystems [4,5,6]. Another more recent endosymbiotic relationship has evolved between plants belonging to distinct lineages of flowering plants (Fabales, Fagales, Cucurbitales, and Rosales) and nitrogen-fixing members of the Burkholderiales, Rhizobiales or Actinomycetales, enabling survival on nitrogen-poor soils. These bacteria fix atmospheric nitrogen under the low oxygen conditions which are provided by plant root nodules.

Studies of mutant legumes deficient in both AM and RNS revealed that a set of genes defined as the common symbiotic signaling pathway (CSSP) are crucial for these symbioses. In the model legume *Lotus japonicus*, Nod factor perception by NFR1 and NFR5 activates downstream signaling through SYMRK, a malectin and leucine-rich repeat (LRR)-containing RLK [7], currently considered to be the first component of the CSSP. SYMRK associates with NFR5 through a mechanism involving intramolecular cleavage of the SYMRK ectodomain, thereby exposing its LRR domains [8]. Signaling from the plasma membrane is transduced to the nuclear envelope where ion channels [9,10], nuclear pore proteins [11,12,13] and cyclic nucleotide-gated channels [14] mediate symbiotic calcium oscillations. These calcium oscillations are interpreted by the calcium- and calmodulin-dependent protein kinase CCaMK, [15,16] that interacts with the DNA binding transcriptional activator CYCLOPS [17,18,19]. Several GRAS transcription factors (NSP1, NSP2, RAM1, RAD1) are activated downstream of CCAMK and CYCLOPS and determine whether plants engage in AMS or RNS symbiosis.

Plants establish the symbioses with AM fungi and nitrogen-fixing bacteria by selecting interacting partners from the taxonomically diverse soil biome. These interactions are driven by low mineral nutrient availability in soil and induce major changes in host and microbial symbiont metabolism [20,21]. Although RNS develops as localized events on legume roots, analysis of *Lotus* mutants impaired in their ability to engage in symbiosis with nitrogen-fixing bacteria revealed that these mutations do not only abrogate RNS, but also impact the composition of taxonomically diverse root- and rhizosphere-associated bacterial communities, indicating an effect on multiple bacterial

taxa that actively associate with the legume host, irrespective of their symbiotic capacity [22]. By contrast, the effect of AMS is known to extend outside the host *via* a hyphal network that can penetrate the surrounding soil and even indirectly affect adjacent plants [23]. In soil, fungal hyphae themselves represent environmental niches and are populated by a specific set of microbes [24]. Although the biology of AMF is well understood, the potential role of AMS on root-associated bacterial and fungal communities is currently unknown.

Here we used mutants impaired in RNS, AM, or both to address the role of symbiosis signaling genes in structuring bacterial and fungal root-associated communities in *Lotus* plants grown in natural soil. We show that genetic disruption of these symbioses results in significant host genotype-dependent microbial community shifts in the root and surrounding rhizosphere compartments. These changes were mainly confined to either bacterial or fungal communities in RNS- or AM-deficient plant lines, respectively, whereas mutants with defects in the CSPP revealed major changes in assemblages of the root microbiota across both microbial kingdoms.

Materials and Methods

Preparation and storage of soil

The soil batches used in this study were collected from Max Planck Institute for Plant Breeding Research agricultural field located in Cologne, Germany (50.958N, 6.865E) in the following seasons: CAS11-spring/autumn 2016, CAS12-spring 2017. The field had not been cultivated in previous years, no fertilizer or pesticide administration took place at the harvesting site. Following harvest, soil was sieved, homogenized and stored at 4 °C for further use.

Soil and plant material

All studied *L. japonicus* symbiosis-deficient mutants, *nfr5-2* [ref. 25], *ram1-2* [ref. 26], *symrk-3* [ref. 7] and *ccamk-13* [ref. 27], originated from the Gifu B-129 genotype.

Plant growth and harvesting procedure

The germination procedure of *L. japonicus* seeds included sandpaper scarification, surface sterilisation in 1% hypochlorite bleach (20 min, 60 rpm), followed by three washes with sterile water and incubation on wet filter paper in Petri dishes for one week (temperature: 20 °C, day/night cycle 16/8h, relative humidity: 60%). For each genotype and soil batch, six to eight biological replicas

99 were prepared by potting four plants in 7x7x9 cm pot filled with corresponding batch of soil (CAS11
100 soil six replicates, CAS12 soil eight replicated). Plants were incubated for ten weeks in the
101 greenhouse (day/night cycle 16/8h, light intensity 6000 LUX, temperature: 20 °C, relative humidity:
102 60%), and were watered with tap water twice per week.

103 The block of soil containing plant roots was removed from the pot and adhering soil was discarded
104 manually. Three sample pools were collected: complete root systems (harvested 1 cm below the
105 hypocotyl), upper fragments of the root systems (4 cm-long, starting 1 cm below the hypocotyl) and
106 lower root system fragments (harvested from 9 cm below; the latter two were collected from plants
107 grown in the same pot (Fig. 1a). All pools were washed twice with sterile water containing 0.02%
108 Triton X-1000 detergent and twice with pure sterile water by vigorous shaking for 1 min. The
109 rhizosphere compartment was derived by collection of pellet following centrifugation of the first
110 wash solution for 10 min at 1500 g. The nodules and visible primordia were separated from
111 washed root pools of nodulating genotypes (WT and ram1-2) with a scalpel and discarded. In order
112 to obtain the root compartment the root sample pools were sonicated to deplete the microbiota
113 fraction attached to the root surface. It included 10 cycles of 30-second ultrasound treatment
114 (Bioruptor NextGen UCD-300, Diagenode) for complete root systems and upper root fragments,
115 while for the lower root fragments the number of cycles was reduced to three. All samples were
116 stored at -80 °C for further processing. For AM colonisation inspection the whole root system of
117 washed soil-grown plants was stained with 5% ink in 5% acetic acid solution and inspected for
118 intraradical infection.

119

120 **Generation of 16S rRNA and ITS2 fragment amplicon libraries for Illumina MiSeq**
121 **sequencing**

122 Root pool samples were homogenized by grinding in a mortar filled with liquid nitrogen and
123 treatment with Precellys24 Tissue lyser (Bertin Technologies) for two cycles at 5600 rpm for 30
124 sec. DNA was extracted with the FastDNA Spin Kit for Soil, according to the manufacturer's
125 protocol (MP Bioproducts). DNA concentrations were measured fluorometrically (Quant-iT™
126 PicoGreen dsDNA assay kit, Life Technologies, Darmstadt, Germany), and adjusted to 3.5 ng/µl.
127 Barcoded primers targeting the variable V5-V7 region of the bacterial 16S rRNA gene (799F and
128 1193R, [28]) or targeting the ITS2 region of the eukaryotic ribosome (fITS7 and ITS4, [29,30]) were

129 used for amplification. The amplification products were purified, pooled and subjected to
130 sequencing with Illumina MiSeq equipment.

131 **Processing of 16S rRNA and ITS2 reads**

132 All libraries from root fractionation experiments as well as from the main experiments were
133 analyzed together. Due to a very low read count for 16S data in the first experiment in CAS11 soil,
134 this library was not included in the final analysis. This resulted in an overall lower sample number
135 for bacteria than for fungi (222 vs. 274 samples). All sets of amplicon reads were processed as
136 recently described [31], using a combination of QIIME [32] and USEARCH tools [33]. For both
137 datasets paired end reads were used. For ITS2 data, forward reads were kept, in case that no
138 paired version was available. Main steps include quality filtering of reads, de-replicating, chimera
139 detection and OTU clustering at a 97% threshold. 16S reads were filtered against the greengenes
140 data base [34], whereas for ITS2 the reads where checked with ITSx [35] and compared against a
141 dedicated ITS database to remove ITS sequences from non-fungal species. Taxonomic
142 classification was done with uclust (assign_taxonomy from QIIME) for 16S OTUs and rdp classifier
143 [36] for ITS2 OTUs. For the sake of consistency with NCBI taxonomic classification, the
144 assignment of the ITS2 sequences was manually corrected so that that all OTUs assigned as
145 Ilyonectria were assigned as belonging to the Sordariomycetes, Hypocreales and Nectriaceae,
146 respectively. For 16S data, OTUs assigned as mitochondrial or chloroplast, were removed prior to
147 analysis.

148 **Statistical analysis**

149 For calculating Shannon diversity indices, OTU tables were rarefied to 1000 reads. Significant
150 differences were determined using ANOVA (aov function in R) and post-hoc Tukey test (TukeyHSD
151 in R, $p<0.05$). For calculating Bray Curtis distances between samples, OTU tables were
152 normalized using cumulative sum scaling (CSS, [37]). Bray-Curtis distances were used as input for
153 principal coordinate analysis (PCoA, cmdscale function in R) plots and as input for constrained
154 analysis of principal coordinate (CPCoA, capscale function, vegan package in R). For the latter, the
155 analysis was constrained by genotypes (each mutant and WT separately) and corrected for the
156 effect of soil type and experiment (using the “Condition” function). This analysis has been repeated
157 with OTU tables from which OTUs that represent known plant symbionts (Phyllobacteriaceae for
158 16S and Glomeromycota for ITS2) were removed before normalization, distance calculation and
159 CPCoA. A previously described approach was used to draw ternary plots and for respective

160 enrichment analysis [22]. Fold change of OTUs between wild type and mutant plants was
161 calculated as followed. Samples showing a read count <5000 were removed. OTUs with mean RA
162 >0.1% across all root or rhizosphere samples, respectively, were kept for analysis. Fold change in
163 RA from WT to mutants was calculated over all WT samples for nfr5-2, ram1-2 and symrk-3,
164 whereas the change to ccamk-13 was only calculated with WT samples from experiments where
165 ccamk-13 mutants were present. To avoid zeros in calculation the RA of OTUs missing from
166 samples was set to 0.001%. The significance of differences in abundance was tested using the
167 Kruskal-Wallis test ($p<0.05$).

168 **Results**

169 **Root fractionation protocol affects the composition of associated bacterial communities**

170 Earlier physiological studies have shown that only cells of a specific developmental stage, located
171 in the root elongation zone, respond to Myc and Nod factors, mount symbiotic calcium oscillations
172 and enable epidermal infection by rhizosphere-derived fungal and bacterial symbionts [38,39].To
173 explore spatial organization of root-associated bacterial and fungal communities along the
174 longitudinal axis, we collected samples of the upper and lower root zones as well as the entire root
175 system of six-week-old Gifu wild-type plants, grown in Cologne soil (2 to 5 cm and >9 cm of the
176 root system, respectively; Fig. 1A; [40]). Microbial assemblages of these three root endosphere
177 compartments were compared to the communities in the corresponding rhizosphere fractions, i.e.
178 soil tightly adhering to the respective root zones, and with the bacterial biome present in unplanted
179 Cologne soil. 16S rRNA gene amplicon libraries of the V5-V7 hypervariable region and gene
180 libraries of the Internally Transcribed Spacer 2 (ITS2) region of the eukaryotic ribosome were
181 generated by amplification [28,29,30]. Information on the number and relative abundance of
182 operational taxonomic units (OTUs) in each compartment was used to calculate α (Shannon index;
183 within sample diversity) and β-diversity (Bray-Curtis distances; between samples diversity), OTU
184 enrichment and taxonomic composition. In bacteria we observed a gradual decrease in α-diversity
185 from unplanted soil to the rhizosphere and to the root endosphere compartments, a trend which
186 was similar for each longitudinal root fraction. This suggests that winnowing of root commensals
187 from the highly complex soil biome occurs in all tested root zones (Fig. S1A). Similar overall results
188 were obtained for the fungal dataset (Fig. S1B), but the decrease in diversity from unplanted soil
189 towards the rhizosphere was mild or even lacking. The latter finding is similar to that of a recent
190 study of root-associated fungi in non-mycorrhizal *A. thaliana* sampled at three natural sites [31].
191 Analyses of taxonomic composition and β-diversity revealed striking differences in the endosphere

192 and rhizosphere compartments associated with the upper and lower root longitudinal fractions. The
193 composition of bacterial and fungal taxa of the whole root closely resembled that of the upper root
194 fraction (Fig. 1B), with only low numbers of OTUs differentially abundant between these two
195 compartments (Fig. 1C and 1D). Additionally, we observed a higher sample-to-sample variation in
196 the taxonomic profiles of the lower root zone compared to the upper whole root fractions (Fig. 1B).
197 This greater community variation in the developmentally younger region of *L. japonicus* roots might
198 reflect a nascent root microbiota or greater variation in root tissue and adherent rhizosphere
199 samples that we recovered from this root zone by our fractionation protocol. Based on the finding
200 that whole root and upper root compartments host comparable bacterial communities and given
201 their greater stability we decided to use the former for further analyses.

202 **Host genes needed for symbioses determine bacterial and fungal community composition**
203 **of *L. japonicus* root and rhizosphere**

204 For root microbiota analysis, we cultivated wild-type (ecotype Gifu) *L. japonicus* and *nfr5-2*, *symrk-*
205 *3*, *ccamk-13* and *ram1-2 (nfr5, symrK, ccamk* and *ram1,* from thereof*)* mutant genotypes in parallel
206 in two batches of Cologne soil, to account for batch-to-batch and seasonal variation at the
207 sampling site. *nfr5-2* mutant plants are impaired in rhizobial Nod factor perception and signaling,
208 which prevents initiation of infection thread formation [25]. Mutations in *SymrK* and *CcamK* affect
209 the common symbiosis pathway downstream of Nod or Myc factor perception, abrogating infection
210 either by nitrogen fixing rhizobia or AM fungi [7,27]. The RAM1 transcription factor controls
211 arbuscule formation, and while *ram1-2* mutants of *L. japonicus* are indistinguishable from wild type
212 and permit incipient AM fungus infection, fungal colonization is terminated with the formation of
213 stunted symbiotic structures [26]. All plant genotypes appeared healthy (Fig. 2A-E), but the shoot
214 length and shoot fresh weight of all mutant plants was significantly reduced in comparison to wild
215 type (Fig. 2F and 2G), suggesting that genetic disruption of either AM or *Rhizobium* symbiosis is
216 detrimental for the fitness of plants grown in natural soil. Whereas all defects in nitrogen-fixing
217 symbiosis, validated by the absence of root nodules in *nfr5-2*, *symrk-3* and *ccamk-13* genotypes
218 (Fig. 2C-E, Table S1), resulted in similarly severe impacts on plant growth (Fig. 2F and 2G), both
219 shoot length and shoot fresh weight were significantly reduced in *ram1-2* plants, although the
220 effects were less severe and these plants still formed nodules and, unlike wild-type and *nfr5-2*,
221 showed impairment in AM symbiosis (Table S1) and a less severe, but significant reduction of both
222 shoot length and shoot fresh weight in comparison to wild type.

223 In order to determine the impact of rhizobial and AM symbiosis on root microbiota assembly, we
224 characterized fungal and bacterial communities of unplanted Cologne soil, rhizosphere, and root
225 compartments of all aforementioned *L. japonicus* genotypes at bolting stage. Visible nodules and
226 root primordia were removed from the roots of nodulating wild type and *ram1*-2 genotypes prior to
227 sample processing for community profiling. We amplified the V5-V7 hypervariable region of the
228 bacterial 16S rRNA gene and the ITS2 region of the eukaryotic ribosome. High-throughput
229 sequencing of these amplicons yielded 22,761,657 16S and 21,228,781 ITS reads, distributed in
230 222 and 274 samples, respectively, which were classified into 5,780 and 3,361 distinct microbial
231 OTUs. Analysis of α-diversity revealed a general reduction of complexity from unplanted soil to
232 rhizosphere and lastly in root compartments for bacterial communities, whereas the complexity of
233 fungal communities was largely similar for the latter two compartments (Fig. S2A and S2B), which
234 is consistent with a recent study of *A. thaliana* root-associated fungal communities [31]. Bacterial
235 α-diversity was slightly elevated in the *nfr5*-2 genotype in rhizosphere and root compartments in
236 comparison to all other genotypes (Fig. S2A). Fungal communities were similarly diverse in the
237 rhizosphere of all tested plant genotypes, but their diversity in the root compartment was
238 significantly and specifically reduced in all three AM mutants (*ccamk*-13, *ram1*-2, and *symrk-3*; Fig.
239 S2B).

240 Analysis of β-diversity using Principal Coordinate Analysis (PCoA) of Bray-Curtis distances
241 showed a significant effect of soil batch on soil-resident bacterial and fungal communities (Fig. S2C
242 and D). In order to account for this technical factor and assess the impact of the different host
243 compartment and genotypes in community composition, we performed a Canonical Analysis of
244 Principle Components Coordinates (CAP; [41]). This revealed a clear differentiation of bacterial
245 and fungal communities in the tested plant genotypes in both root and rhizosphere compartments,
246 with the host genotype explaining as much as 7.61% of the overall variance of the 16S rRNA, and
247 13.5% of ITS2 data (Fig. 3; $P<0.001$). The rhizosphere compartments of wild type and *ram1-2* were
248 found to harbor similar bacterial communities, but were separate from those of *symrk-3* and
249 *ccamk-13* (Fig. 3A). Further, the rhizosphere communities of each of these four plant genotypes
250 were found to be significantly different from that of *nfr5* (Fig. 3A). A similar trend was observed for
251 fungal communities, except that wild-type and *ram1* rhizosphere communities were clearly
252 separated from each other (Fig. 3C). In the root compartment we found bacterial consortia that
253 were distinctive for each of the five plant genotypes (Fig. 3B). A pronounced host genotype effect
254 was also found for the root-associated fungal communities, but in this case the communities of
255 wild-type and *nfr5* clustered together, indicating a high similarity (Fig. 3D). *L. japonicus* is

256 nodulated by members of *Mesorhizobium loti* belonging to the Phyllobacteriaceae family, and
257 engages in AM symbiosis with Glomeromycota fungi. The plant genotypes included in this study
258 differed in their capacity to accommodate nitrogen-fixing bacteria and/or AM fungi inside roots,
259 and, consequently, the lack of these symbionts alone might explain the microbial community
260 separation observed by CAP analysis (Fig. 3). To test whether these symbiotic microbes are the
261 sole drivers of the observed community separations, we repeated the CAP analysis after *in silico*
262 removal of *Phyllobacteriaceae* sequencing reads for bacterial communities, and of Glomeromycota
263 reads for the fungal assemblages. Interestingly, although this reduced the community variance
264 explained by host genotype across the dataset (Fig. S3 compared to Fig. 3), overall patterns of β-
265 diversity remained unaltered, suggesting that other community members besides root nodule and
266 arbuscular mycorrhizal symbionts contribute to the plant genotype-specific community shifts.
267 Collectively, our analyses of *L. japonicus* symbiotic mutants grown in natural soil show that lack of
268 AM and/or RNS symbioses has a significant effect on plant growth and on the structures of
269 bacterial and fungal communities associated with legume roots.

270 **Loss of symbiosis affects specific bacterial and fungal families of the root microbiota**

271 Comparison of bacterial family abundance between wild type and mutants lacking RNS and/or AM
272 symbiosis identified significant changes in *Comamonadaceae*, *Phyllobacteriaceae*,
273 *Methylophilaceae*, *Cytophagaceae* and *Sinobacteracea* in the rhizosphere compartment (Fig. 4A;
274 top 10 most abundant families). The abundance of *Comamonadaceae* and *Phyllobacteriaceae*
275 also differed significantly in the root compartment of RNS mutants compared to wild type.
276 *Streptomycetaceae* and *Sinobacteraceae* relative abundances were specifically affected by loss of
277 *Nfr5*, whereas *Anaeroplamataceae* and *Burkholderiaceae* abundances were affected by the lack of
278 AM symbiosis in *symrk* and *ccamk* plants (Fig. 4A). The relative abundances of the same two
279 families were also significantly reduced in *ram1* roots, suggesting that active AM symbiosis
280 influences root colonization by a subset of bacterial root microbiota taxa.

281 Six out of the ten most abundant fungal families in the rhizosphere compartment of *Lotus* plants
282 belonged to Ascomycota (Fig. 4B). By contrast, the root endosphere was dominated by numerous
283 families of Glomeromycota, which were found to be almost fully depleted from the rhizosphere and
284 root compartments of *ram1*, *symrk* and *ccamk* mutants, indicating that absence of AM symbiosis
285 predominantly affects Glomeromycota and does not limit root colonization or rhizosphere
286 association by other fungal families. However, depletion of Glomeromycota in the AM mutant roots
287 was accompanied by an increase in the relative abundance of Ascomycota members belonging to

288 *Nectriaceae* in both rhizosphere and root compartments and by an increased abundance of
289 unclassified *Helotiales*, *Leotiomycetes*, and *Sordariomycetes* in the root compartment only (Fig.
290 4B).

291 Closer inspection of the microbial community shifts at the OTU level identified 45 bacterial OTUs
292 and 87 fungal OTUs enriched in the roots of symbiosis mutants compared to those of wild type
293 (Fig. 5), and 60 bacterial OTUs and 30 differentially abundant fungal OTUs in the rhizosphere
294 samples (Fig. S4). The absence of RNS in *nfr5-2* roots affected the relative abundance of multiple
295 OTUs (n=27 in the root, n=23 in the rhizosphere) belonging to diverse taxa. Many of these OTUs
296 (n=18 in the root, n=16 in the rhizosphere) showed a similar differential relative abundance in
297 *symrk-3* and/or *ccamk-13* mutants when compared to wild type (Fig.5A), indicating that their
298 contribution to the *Lotus* root communities outside of nodules is affected by active nitrogen fixing
299 symbiosis. Impairment of both AM and RNS symbioses in *symrk* and/or *ccamk* mutants resulted in
300 opposite changes in the relative root abundances of OTUs belonging to specific Burkholderiales
301 families. Depletion of OTUs belonging to *Burkholderiaceae* (n=5) was accompanied by the
302 enrichment of OTUs from other Burkholderiales families (*Oxalobacteraceae* [n=3],
303 *Comamonadadaceae* [n=2], and *Methylophilaceae* [n=2]; Fig. 5A). Only three of the above-
304 mentioned *Burkholderiaceae* OTUs were depleted in *ram1* roots, suggesting that their enrichment
305 in *Lotus* roots is dependent on functional AM symbiosis.

306 Analysis of the ITS2 amplicon sequences from root samples identified a large number of
307 Glomeromycota OTUs (n=39); thus, *Lotus* Gifu roots grown in natural soil accommodate a
308 phylogenetically diverse community of AM fungi (Fig. 5B). The majority of these fungal OTUs
309 (n=31) were depleted in *symrk-3*, *ccamk-13* and *ram1-2* mutant roots, indicating that their
310 enrichment is dependent on a functional AM symbiosis pathway. Their intraradical colonization
311 appears to be independent of *RAM1*, as 12 OTUs assigned to Glomeromycota or to unknown taxa,
312 nine of which define a Glomeromycota sublineage, were depleted in *symrk-3* and *ccamk-13* but not
313 in *ram1-2* roots. A reduced abundance of Glomeromycota OTUs in the endosphere compartment
314 was accompanied by an increased abundance of Ascomycota members, especially of members
315 belonging to the *Nectriaceae* (8 OTUs) and *Helotiales* (7 OTUs) families, suggestive of a mutually
316 exclusive occupancy of the intraradical niche. In sum, our results reveal that in natural soil CSSP
317 symbiotic genes are essential for root colonization by a wide range of Glomeromycota fungi;
318 further, these genes significantly affect the abundances of multiple bacterial taxa, predominantly
319 belonging to the Burkholderiales and Rhizobiales orders.

320 **Discussion**

321 Here, we investigated the role of host AM and/or RNS genes in establishing structured bacterial
322 and fungal communities in the rhizosphere and endosphere compartments of *L. japonicus* grown in
323 natural soil. Impairment of RNS in *nfr5-2* or AMS in *ram1-2* plants had a significant impact on root
324 microbiota structure, which was mainly confined to the composition of bacterial or fungal
325 communities, respectively.

326 The shift between the root-associated microbial communities of wild type and *nfr5-2* mutant is in
327 line with both the qualitative and quantitative findings of a previous report on the *Lotus* bacterial
328 root microbiota (Fig. 3A and B in this study; [22]). However, here we observed an enhanced
329 rhizosphere effect in both wild type and *nfr5-2* plants, leading also to a less prominent community
330 shift in this compartment (Fig. S5). These differences in rhizosphere bacterial composition are
331 likely caused by a soil batch effect and, to a lesser extent, possibly also the use of different
332 sequencing platforms (Illumina *versus* 454 pyrosequencing). The nearly unaltered fungal
333 community composition in *nfr5* mutant plants compared to wild type (only 3 out of 39
334 Glomeromycota OTUs differentially abundant) suggests that NFR5 is dispensable for fungal
335 colonization of *L. japonicus* roots. This finding, together with a massive shoot biomass reduction of
336 *nfr5* plants in natural soil (~4-fold; Fig. 2), further reveals that intraradical colonization by soil-
337 derived fungal endophytes is robust against major differences in plant growth.

338 A recent microbial multi-kingdom interaction study in *A. thaliana* showed that bacterial commensals
339 of the root microbiota are crucial for the growth of a taxonomically wide range of fungal root
340 endophytes. These antagonistic interactions between bacterial and fungal root endophytes are
341 essential for plant survival in natural soil [31]. We have shown here that an almost complete
342 depletion of diverse Glomeromycota taxa from roots of each of the three AM mutants was
343 accompanied by an enrichment of OTUs belonging to the families *Nectriaceae* and Helotiales (Fig.
344 4). We speculate that the increased relative abundance of these taxa is caused by intraradical
345 niche replacement as a compensatory effect following the exclusion of Glomeromycota symbionts
346 from the root compartment. Previous mono-association experiments have shown that isolates
347 belonging to *Nectriaceae* and Helotiales can have either mutualistic or pathogenic phenotypes
348 [42,43,44]. Given that all plant genotypes were free of disease symptoms when grown in natural
349 soil (Fig. 2), we speculate that the complex shifts in the composition of the bacterial root microbiota
350 in *nfr5-2, symRK-3,* and *ccamk-13* mutants did not affect the capacity of bacterial endophytes to
351 prevent pathogenic fungal overgrowth. Of note, Helotiales root endophytes were also enriched in

352 roots of healthy *Arabis alpina*, a non-mycorhyzal plant species and relative of *A. thaliana*, and
353 contribute to phosphorus nutrition of the host when grown in extremely phosphorus-impoverished
354 soil [45]. The enrichment of Helotiales in *Lotus* AM mutants is therefore consistent with potential
355 niche replacement by other fungal lineages to ensure plant nutrition in nutrient-impoverished soils.
356 Although the proposed compensatory effect in AM mutants will need further experimental testing in
357 phosphorus-depleted soils, our hypothesis is consistent with the only mild impairment in plant
358 growth in *ram1-2* mutants (Fig. 2).

359 We identified three bacterial OTUs, all belonging to the *Burkholderiaceae* family, that are
360 significantly depleted in the roots of each of the three AM mutants compared to wild type.
361 Interestingly, members of the Glomeromycota have been found to contain intracellular
362 endosymbiotic bacteria [46], some belonging to the order Burkholderiales [47]. This finding
363 suggests that these bacteria are either endosymbionts of Glomeromycota fungi that are excluded
364 from the roots of the AM defective genotypes or that their intraradical colonization is indirectly
365 mediated by AM infection. The small changes in the bacterial root microbiota in *ram1-2* plants,
366 which were mainly limited to depletion of the three aforementioned Burkholderia OTUs, revealed
367 that root-associated bacterial community structure is remarkably robust against major changes in
368 the composition of root-associated fungal communities (Fig. 5).

369 Paleontological and phylogenomic studies established the ancestral origin of genetic signatures
370 enabling AM symbiosis in land plants [1,48]. In monocots and dicots, the extended AM fungal
371 network is primarily recognized as a provider of nutrients, particularly phosphorus [49,50], but the
372 positive impact of AM symbiosis on the host transcends nutrient acquisition [51]. Additionally,
373 phylogenomic studies of the symbiotic phosphate transporter PT4 suggest that this trait evolved
374 late and therefore that phosphorus acquisition might not have been the (only) driving force for the
375 emergence of AM symbiosis [48]. *SymRK* and *Ram1* were identified in the genomes of liverworts,
376 but evolution of *CCaMK* predated the emergence of all land plants, as shown by its presence and
377 conserved biochemical function in advanced charophytes [48]. Together, these findings raise
378 questions regarding the forces driving the evolution of signaling genes enabling intracellular
379 symbioses in land plants. Our study shows that in *L. japonicus*, simultaneous impairment of AM
380 and RN symbioses in *symRK-3* and *ccamk*-13 plants had a dramatic effect on the composition of
381 both bacterial and fungal communities of the legume root microbiota (Fig. 5). Importantly, mutation
382 of *CcamK* and *SymrK* led to an almost complete depletion of a large number of fungal OTUs,
383 mostly belonging to Glomeromycota, indicating that in *Lotus*, these genes predominantly control

384 the colonization of roots by this particular fungal lineage. The finding that *ram1-2* mutants show
385 retained accommodation for a subset of fungal root endophytes (n=13; Fig. 5B, and Fig 4B) whose
386 colonization is dependent on an intact common symbiosis pathway is not surprising based on the
387 capacity of these mutants to enable fungal colonization but not to sustain a full symbiotic
388 association [26], and indicates that *RAM1* is dispensable for the intraradical colonization of these
389 Glomeromycota fungi. Alternatively, these fungal root endophytes may engage in commensal
390 rather than mutualistic relationships with *L. japonicus* independently of the AM symbiosis pathway
391 as is the case for multiple species of commensal non-symbiotic rhizobia [22,52]. For instance,
392 given that *ram1*-2 mutants specifically block AM arbuscule differentiation but not root colonisation
393 [26], it is conceivable that the Glomeromycota taxa colonizing this plant genotype may not form
394 arbuscules during root colonization.

395 Legumes have evolved the capacity to recognize and accommodate both types of intracellular
396 symbionts, and the large effect of CSSP genes on associated microbiota seen in the present work
397 could reflect a legume-specific trait. However, in rice, which does not engage in symbiotic
398 relationships with nodulating rhizobia, mutants lacking *CCaMK* were also found to display
399 significant changes in root-associated bacterial communities that could be mainly explained by
400 depletion of Rhizobiales and Sphingomonadales lineages [53]. Thus, our findings based on
401 comparative microbiota analysis of *Lotus ccamk* and *ram1* mutants suggest a broader role for
402 common symbiosis signaling genes in microbiota assembly. Future studies on orthologous genes
403 in basal land plants will contribute to a better understanding of the role of symbiotic signaling in the
404 evolution of plant-microbiota associations.

405

Acknowledgements

This work was supported by funds to S. R. from The Danish National Research Foundation (Grant no. DNRF79), by funds to P.S.-L. from the Max Planck Society, a European Research Council advanced grant (ROOTMICROBIOTA), the 'Cluster of Excellence on Plant Sciences' program funded by the Deutsche Forschungsgemeinschaft (DFG), and SPP 2125 DECRyPT from the DFG.

Conflict of interest

The authors declare no conflict of interests.

Data availability

All sequencing reads will be uploaded to the European Nucleotide Archive (ENA). Code and relevant data files (e.g. OTU tables) will be made public via GitHub.

418 **References**

419 1. Remy W, Taylor TN, Hass H, Kerp H. Four hundred-million year-old vesicular arbuscular
420 mycorrhizae. *Proc Natl Acad Sci USA* 91 1994; 11:841–11.

421 2. Taylor TN, Remy W, Hass H, Kerp H. Fossil Arbuscular Mycorrhizae from the Early Devonian.
422 *Mycologia* 1995; 87(4):560-573.

423 3. Pirozynski KA, Malloch DW. The origin of land plants: a matter of mycotrophism. *Biosystems*
424 1975; 6:153-164.

425 4. Smith SE, Read D J,Vesicular-arbuscular mycorrhizas in agriculture and horticulture. In
426 *Mycorrhizal Symbiosis* . Academic press,1997. (pp. 453-469).

427 5. Wang B, Qiu YL. Phylogenetic distribution and evolution of mycorrhizas in land plants.
428 *Mycorrhiza* 2006; 16(5):299-363.

429 6. Bonfante P, Genre A. Mechanisms underlying beneficial plant-fungus interactions in mycorrhizal
430 symbiosis. *Nat Commun* 2010; 1:48.

431 7. Stracke S, Kistner C, Yoshida S, Mulder L, Sato S, Kaneko T, et al. A plant receptor-like kinase
432 required for both bacterial and fungal symbiosis. *Nature* 2002; 417(6892):959-62

433 8. Antolin-Llovera M, Ried MK, Parniske M. Cleavage of the SYMBIOSIS RECEPTOR-LIKE
434 KINASE ectodomain promotes complex formation with Nod factor receptor 5. *Curr Biol* 2014;
435 24(4):422-427.

436 9. Charpentier M, Bredemeier R, Wanner G, Takeda N, Schleiff E, Parniske M. Lotus japonicus
437 CASTOR and POLLUX are ion channels essential for perinuclear calcium spiking in legume root
438 endosymbiosis. *Plant Cell* 2008; 20(12).

439 10. Ane JM, Kiss GB, Riely BK, Penmetsa RV, Oldroyd GE, Ayax C. Medicago truncatula DMI1
440 required for bacterial and fungal symbioses in legumes. *Science* 2004; 303(5662):1364-1367.

441 11. Kanamori N, Madsen LH, Radutoiu S, Frantescu M, Quistgaard EM, Miwa H. A nucleoporin is
442 required for induction of Ca2+ spiking in legume nodule development and essential for rhizobial
443 and fungal symbiosis. *Proc Natl Acad Sci* USA 2006; 103(2):59-364

444 12. Saito K, Yoshikawa M, Yano K, Miwa H, Uchida H, Asamizu E. NUCLEOPORIN85 is
445 required for calcium spiking, fungal and bacterial symbioses, and seed production in Lotus
446 japonicus. *Plant Cell* 2007; 19(2):610-624

447 13. Groth M, Takeda N, Perry J, Uchida H, Draxl S, Brachmann A. NENA, a Lotus japonicus
448 homolog of Sec13, is required for rhizodermal infection by arbuscular mycorrhiza fungi and
449 rhizobia but dispensable for cortical endosymbiotic development. *Plant Cell* 2010; 22(7):2509-
450 2526.

451

452 14. Charpentier M, Sun J, Vaz Martins T, Radhakrishnan GV, Findlay K, Soumpourou E. Nuclear-
453 localized cyclic nucleotide-gated channels mediate symbiotic calcium oscillations. Science 2016;
454 352(6289):1102-1105.

455 15. Levy J, Bres C, Geurts R, Chalhoub B, Kulikova O, Duc G. A putative Ca2+ and calmodulin-
456 dependent protein kinase required for bacterial and fungal symbioses. Science 2004;
457 303(5662):1361-1364.

458 16. Mitra RM, Gleason CA, Edwards A, Hadfield J, Downie JA, Oldroyd GE, et al. A
459 Ca2+/calmodulin-dependent protein kinase required for symbiotic nodule development: Gene
460 identification by transcript-based cloning. *Proc Natl Acad Sci U S A* 2004; 101(13):4701-5.

461 17. Yano K, Yoshida S, Muller J, Singh S, Banba M, Vickers K. et al. CYCLOPS, a mediator of
462 symbiotic intracellular accommodation. *Proc Natl Acad Sci U S A* 2008; 105(51):20540-20545.

463 18. Singh S, Katzer K, Lambert J, Cerri M, Parniske M. CYCLOPS, a DNA-binding transcriptional
464 activator, orchestrates symbiotic root nodule development. *Cell Host Microbe* 2014; 15(2):139-152.

465 19. Messinese E, Mun JH, Yeun LH, Jayaraman, D, Rouge P, Barre, A, et al. A novel nuclear
466 protein interacts with the symbiotic DMI3 calcium- and calmodulin-dependent protein kinase of
467 Medicago truncatula.. *Mol Plant Microbe Interact* 2007; 20(8):912-921.

468 20. Udvardi M, Poole PS. Transport and metabolism in legume-rhizobia symbioses. *Annu Rev Plant*
469 *Biol* 2013; 64:781-805.

470 21. Gutjahr C, Sawers RJH, Marti G, Andres-Hernandez L, Yang S, Casieri L. Transcriptome
471 diversity among rice root types during asymbiosis and interaction with arbuscular mycorrhizal
472 fungi. *Proc Natl Acad Sci* USA 2015; 112(21):6754.

473 22. Zgadzaj R, Garrido-Oter R, Jensen DB, Koprivova A, Schulze-Lefert P, Radutoiu S. Root
474 nodule symbiosis in Lotus japonicus drives the establishment of distinctive rhizosphere, root, and
475 nodule bacterial communities. *Proc Natl Acad Sci U S A* 2016; 113(49):E7996-E8005.

476 23. Johnson D, Gilbert L. Interplant signalling through hyphal networks. New Phytol 2014;
477 205(4):1448-53.

478 24. Hassani MA, Duran, P, Hacquard S. Microbial interactions within the plant holobiont.
479 *Microbiome* 2018; 6(1):58.

480 25. Madsen EB, Madsen, LH, Radutoiu S, Olbryt M, Rakwalska M, Szczyglowski K, et al. A
481 receptor kinase gene of the LysM type is involved in legumeperception of rhizobial signals. *Nature*
482 2003; 425(6958):637.

483 26. Xue L, Cui H, Buer B, Vijayakumar V, Delaux PM, Junkermann S, et al. Network of GRAS
484 transcription factors involved in the control of arbuscule development in Lotus japonicus. *Plant*
485 *Physiol* 2015; 167(3):854-871.

486

487 27. Perry J, Brachmann A, Welham T, Binder A, Charpentier M, Groth M, et al. TILLING in Lotus
488 japonicus identified large allelic series for symbiosis genes and revealed a bias in functionally
489 defective ethyl methanesulfonate alleles toward glycine replacements. *Plant Physiol* 2009; 151:
490 1281–1291.

491 28. Schlaeppi K, Dombrowski N, Oter RG, Ver Loren van Themaat E, Schulze-Lefert P.
492 Quantitative divergence of the bacterial root microbiota in Arabidopsis thaliana relatives. *Proc Natl*
493 *Acad Sci U S A* 2014; 111(2):585-92.

494 29. Ihrmark K, Bödeker IT, Cruz-Martinez K, Friberg H, Kubartova A, Schenck J,et al. New
495 primers to amplify the fungal ITS2 region--evaluation by 454-sequencing of artificial and natural
496 communities. *FEMS Microbiol Ecol* 2012; 82(3):666-77.

497 30. White TJ, Bruns TD, Lee SB, Taylor JW. Amplification and direct sequencing of fungal
498 ribosomal RNA genes for phylogenetics. In: Innis MA, Gelfand DH, Sninsky JJ, White TJ, editors.
499 *PCR protocols: a guide to methods and applications*. United States: Academic Press, CA, USA,
500 1990, pp. 315-322.

501 31. Duran, P., Thiergart T, Garrido-Oter R, Agler M, Kemen E, Schulze-Lefert P, et al. (2018).
502 Microbial interkingdom interactions in roots promote Arabidopsis survival. *Cell* 2018; 175(4):973-
503 983.

504 32. Caporaso JG, Kuczynski J, Stombaugh J, Bittinger K, Bushman FD, Costello EK, et al. QIIME
505 allows analysis of high-throughput community sequencing data. *Nat Methods* 2010; 7:335-336.

506 33. Edgar RC. UPARSE: highly accurate OTU sequences from microbial amplicon reads. *Nat*
507 *Methods* 2013; 10:996-998.

508 34. DeSantis TZ, Hugenholtz P, Larsen N, Rojas M, Brodie EL, Keller K, et al. Greengenes, a
509 chimera-checked 16S rRNA gene database and workbench compatible with ARB. *Appl Environ*
510 *Microbiol* 2006; 72:5069-5072

511 35. Bengtsson-Palme J, Ryberg M, Hartmann M, Branco S, Wang Z, Godhe A, De Wit P, et al.
512 Improved software detection and extraction of ITS1 and ITS2 from ribosomal ITS sequences of
513 fungi and other eukaryotes for analysis of environmental sequencing data. *Methods Ecol Evol* 2013;
514 4: 914-919.

515 36. Wang Q, Garrity GM, Tiedje JM, Cole JR. Naive Bayesian classifier for rapid assignment of
516 rRNA sequences into the new bacterial taxonomy. *Appl Environ Microb* 2007; 73:5261-5267.

517 37. Paulson, JN, Stine, OC, Bravo HC, Pop M. Differential abundance analysis for microbial
518 marker-gene surveys. *Nat Methods* 2013; 10:1200-1202.

519 38. Chabaud M, Genre A, Sieberer BJ, Faccio A, Fournier J, Novero M, et al. Arbuscular
520 mycorrhizal hyphopodia and germinated spore exudates trigger Ca2+ spiking in the legume and
521 nonlegume root epidermis. *New Phytol* 2011; 189(1):347-5.

522

523 39. Miwa H, Sun J, Oldroyd GE, Downie JA. Analysis of calcium spiking using a cameleon
524 calcium sensor reveals that nodulation gene expression is regulated by calcium spike number and
525 the developmental status of the cell. *Plant J* 2006; 48(6):883-94.

526 40. Bulgarelli D, Rott M, Schlaeppi K, Emiel Ver Loren van Themaat E, Ahmadinejad N, Assenza
527 F, et al. Revealing structure and assembly cues for Arabidopsis root-inhabiting bacterial microbiota.
528 *Nature* 2012; 488:91-95.

529 41. Anderson MJ, Willis TJ, Canonical analysis of principal coordinates: A useful method of
530 constrained ordination for ecology. *Ecology* 2003; 84(2):511-525.

531 42. Lombard L, van der Merwe NA, Groenewald JZ, Crous PW. Generic concepts in Nectriaceae.
532 *Stud Myco*l 2015; 80:189-245.

533 43. Lofgren LA, LeBlanc NR, Certano AK, Nachtigall J, LaBine KM, Riddle J, et al. Fusarium
534 graminearum: pathogen or endophyte of North American grasses? *New Phytol* 2018; 217(3):1203-
535 1212.

536 44. Amselem J, Cuomo CA, van Kan, JA, Viaud M, Benito EP, Couloux A, et al. Genomic analysis
537 of the necrotrophic fungal pathogens Sclerotinia sclerotiorum and Botrytis cinerea. *PLoS Genet*
538 2011; 7(8).

539 45. Almario J, Jeena G, Wunder J, Langen G, Zuccaro A, Coupland G, Bucher M. Root-associated
540 fungal microbiota of nonmycorrhizal Arabis alpina and its contribution to plant phosphorus
541 nutrition. *Proc Natl Acad Sci U S A* 2017; 114(44):E9403-E9412.

542 46. Desiro A, Salvioli A, Ngonkeu EL, Mondo SJ, Epis S, Faccio A, et al. Detection of a novel
543 intracellular microbiome hosted in arbuscular mycorrhizal fungi. *ISME J* 2014; 8(2): 257-270.

544 47. Bianciotto V, Lumini E, Lanfranco L, Minerdi D, Bonfante P, Perotto S. Detection and
545 identification of bacterial endosymbionts in arbuscular mycorrhizal fungi belonging to the family
546 Gigasporaceae. *Appl Environ Microbiol* 2000;66(10):4503-4509.

547 48. Delaux PM, Radhakrishnan GV, Jayaraman D, Cheema J, Malbreil M, Volkening JD,et al.
548 Algal ancestor of land plants was preadapted for symbiosis. *Proc Natl Acad Sci U S A* 2015;
549 112(43):13390-13395.

550 49. Javot H, Penmetsa RV, Terzaghi N, Cook DR, Harrison MJ. A Medicago truncatula phosphate
551 transporter indispensable for the arbuscular mycorrhizal symbiosis. *Proc Natl Acad Sci U S A* 2007;
552 104(5):1720-5.
553
554 50. Sawers RJ, Svane SF, Quan C, Grønlund M, Wozniak B, Gebreselassie MN, et al. Phosphorus
555 acquisition efficiency in arbuscular mycorrhizal maize is correlated with the abundance of root-
556 external hyphae and the accumulation of transcripts encoding PHT1 phosphate transporters. *New*
557 *Phytol* 2017; 214(2):632-643.
558
559 51. Chen M, Arato M, Borghi L, Nouri E, Reinhardt D. Beneficial Services of Arbuscular
560 Mycorrhizal Fungi - From Ecology to Application. *Front Plant Sci* 2018; 9:1270.

52. Garrido-Oter R, Nakano RT, Dombrowski N, Ma KW, AgBiome T, McHardy AC, et al. Modular Traits of the Rhizobiales Root Microbiota and Their Evolutionary Relationship with Symbiotic Rhizobia. *Cell Host Microbe* 2018; 24(1):155-167 e155.

53. Ikeda S, Okubo T, Takeda N, Banba M, Sasaki K, Imaizumi-Anraku H, et al. The genotype of the calcium/calmodulin-dependent protein kinase gene (CCaMK) determines bacterial community diversity in rice roots under paddy and upland field conditions. *Appl Environ Microbiol* 2011; 77(13):4399-4405.

Main Figures

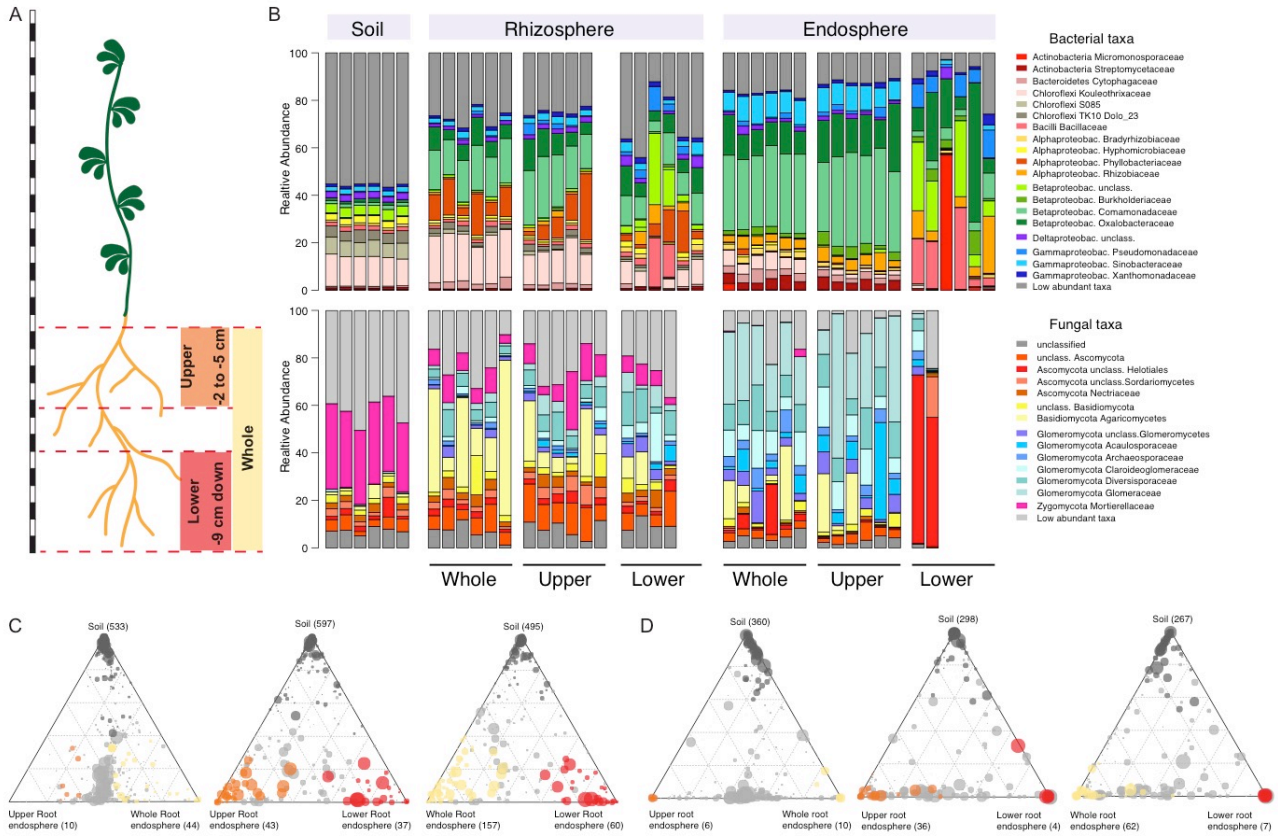

Fig1, **Bacterial & fungal community profile for different root fractions of *L. japonicus***.
A) Cartoon showing the length of the three different root fractions. B) Community profile showing the relative abundance of bacterial (upper panel) and fungal (lower panel) families across compartments and fractions (only samples with >5000 (bacteria) or >1000 (fungi) reads are shown, taxa having average RA < 0.1 (bacteria) or <0.15 (fungi) across all samples are aggregated as low-abundant.). C) Ternary plots showing bacterial OTUs that are enriched in the endosphere of specific root fractions, compared to the soil samples. B) Ternary plots showing fungal OTUs that are enriched in the endosphere of specific root fractions, compared to the soil samples. Circle size corresponds to RA across all fractions. Dark grey circles denote OTUs that are enriched in soil, light grey circles always represent OTUs that are not enriched in any of the fractions.

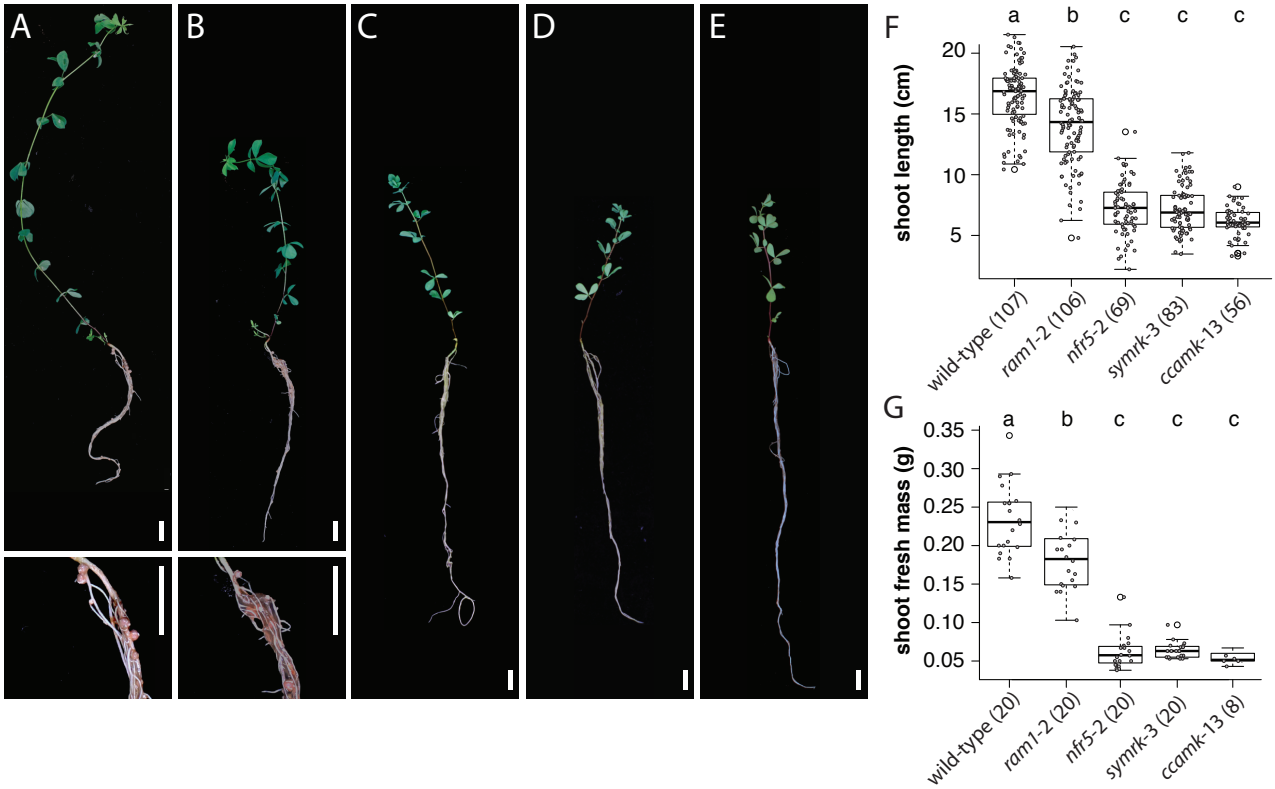

Fig2, **Phenotypes of WT and mutant plants**. Images depicting *L. japonicus* wild-type (A) and symbiosis-deficient mutant plants: *ram1-2* (B), *nfr5-2* (C), *symRK-3* (D) and *ccamk-13* (E). Insets show close-up view of nodules. Scale bars correspond to 1 cm. F) Boxplots display the shoot length for the identical set of genotypes presented in (A-E). G) Boxplots displaying the shoot fresh mass. Letters above plots correspond to groups based on Tukey's HSD test ($P<0.05$). Number of samples are indicated in brackets.

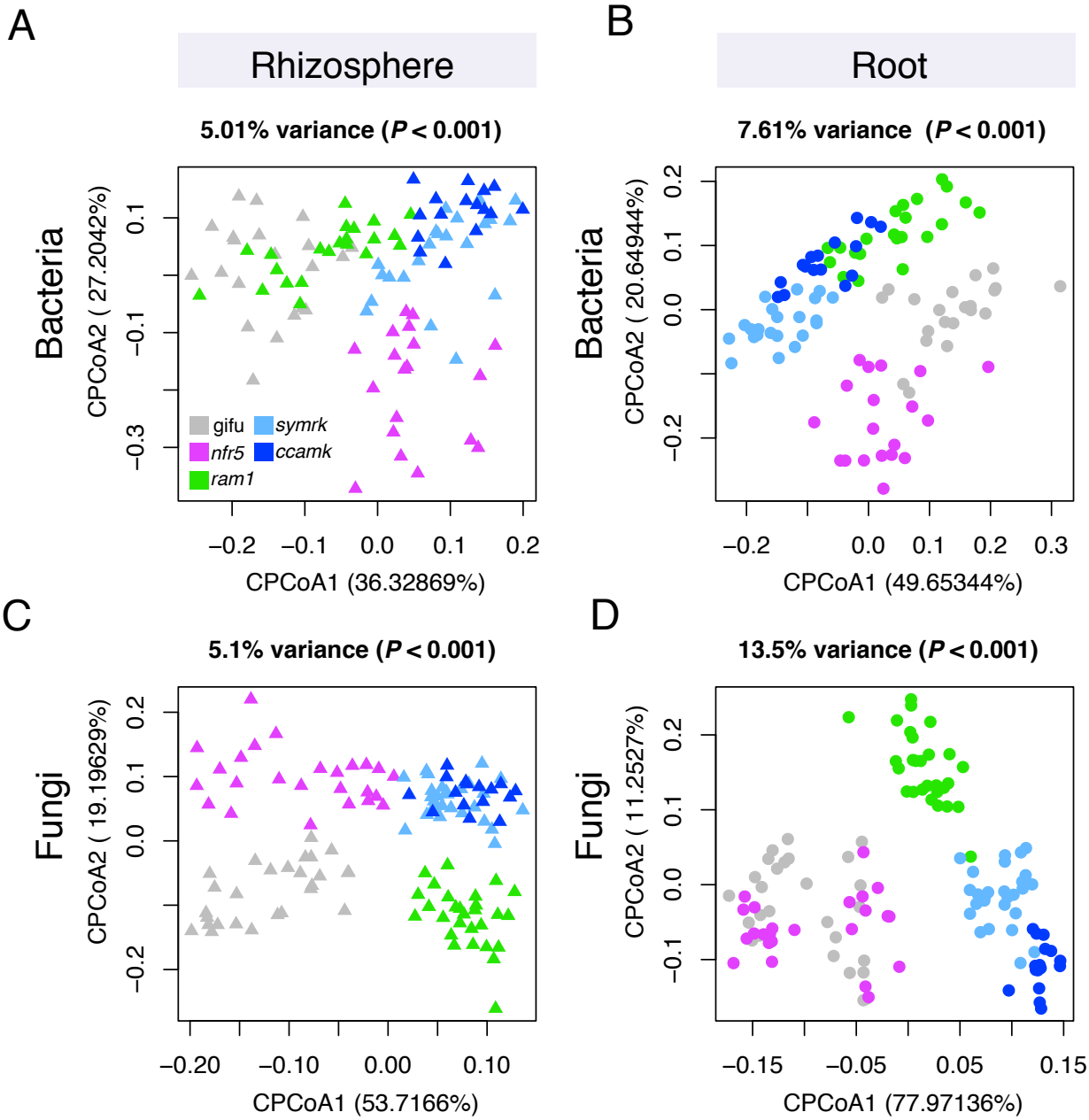

Fig3, **Constrained PCoA analysis showing genotype effect on microbial communities.** A) Constrained PCoA plots for bacterial datasets showing rhizosphere samples (n = 100) and B) root samples (n = 100). C) Constrained PCoA plots for fungal datasets showing only rhizosphere samples (n = 124) and D) root samples (n = 122).

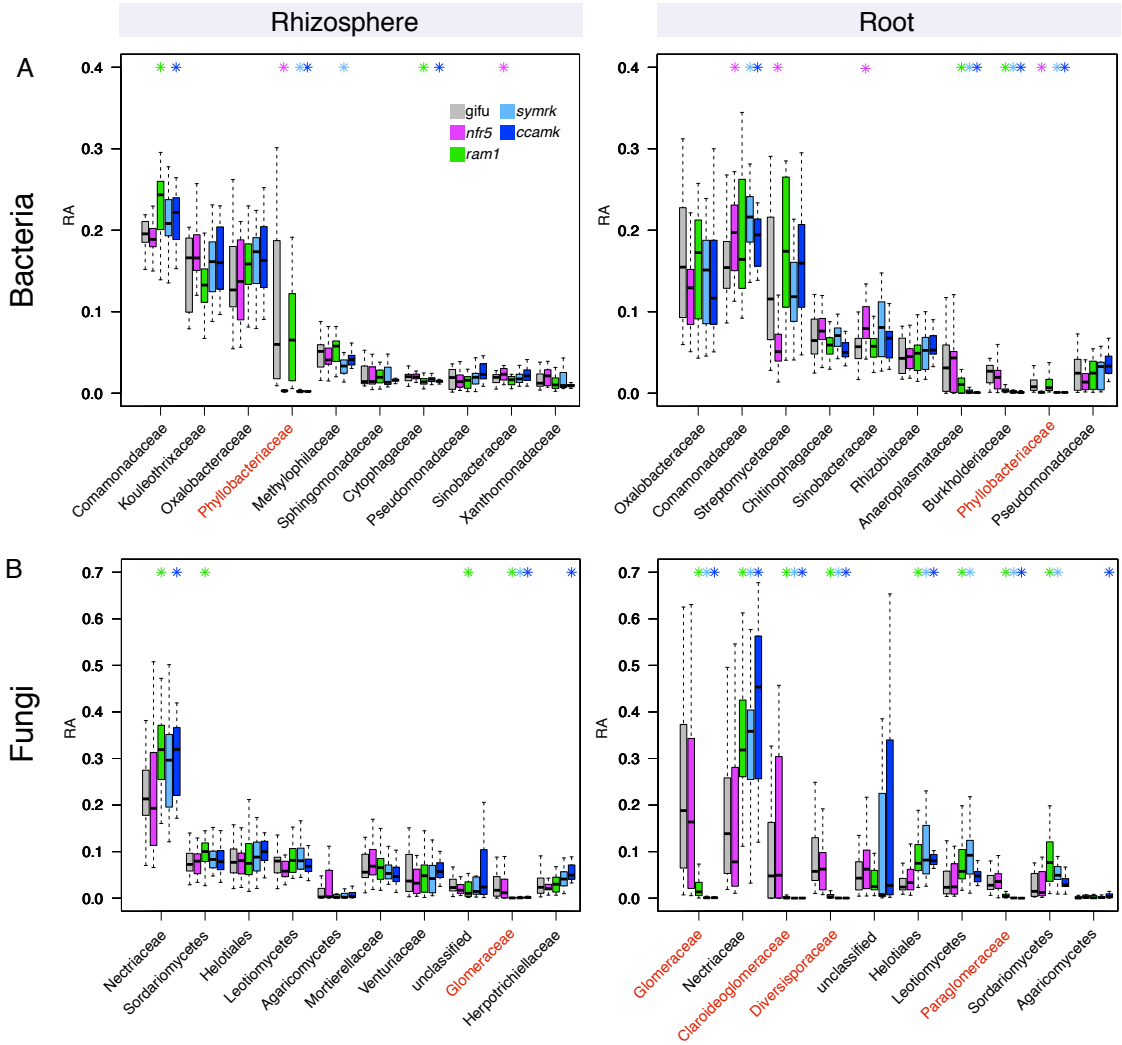

Fig4, **Relative abundance for main microbial taxa across plant compartments and genotypes**. A) RA for bacterial families in rhizosphere (left panel) and root compartment (right panel). B) RA for fungal families in rhizosphere (left panel) and root compartment (right panel). Taxa are sorted in decreasing order according to their average RA in wt plants (only first 10 most abundant taxonomical groups are shown). RA in wt as well as in the respective mutants is displayed. Significant differences compared to wt are marked with an asterisk in the color of the mutant ($P<0.05$, Kruskal-Wallis test). Families that include known symbionts are marked in red (Phyllobacteriaceae for bacteria and Glomeromyctes for Fungi). For some fungal taxa the next higher rank is shown, when no family level information was available.

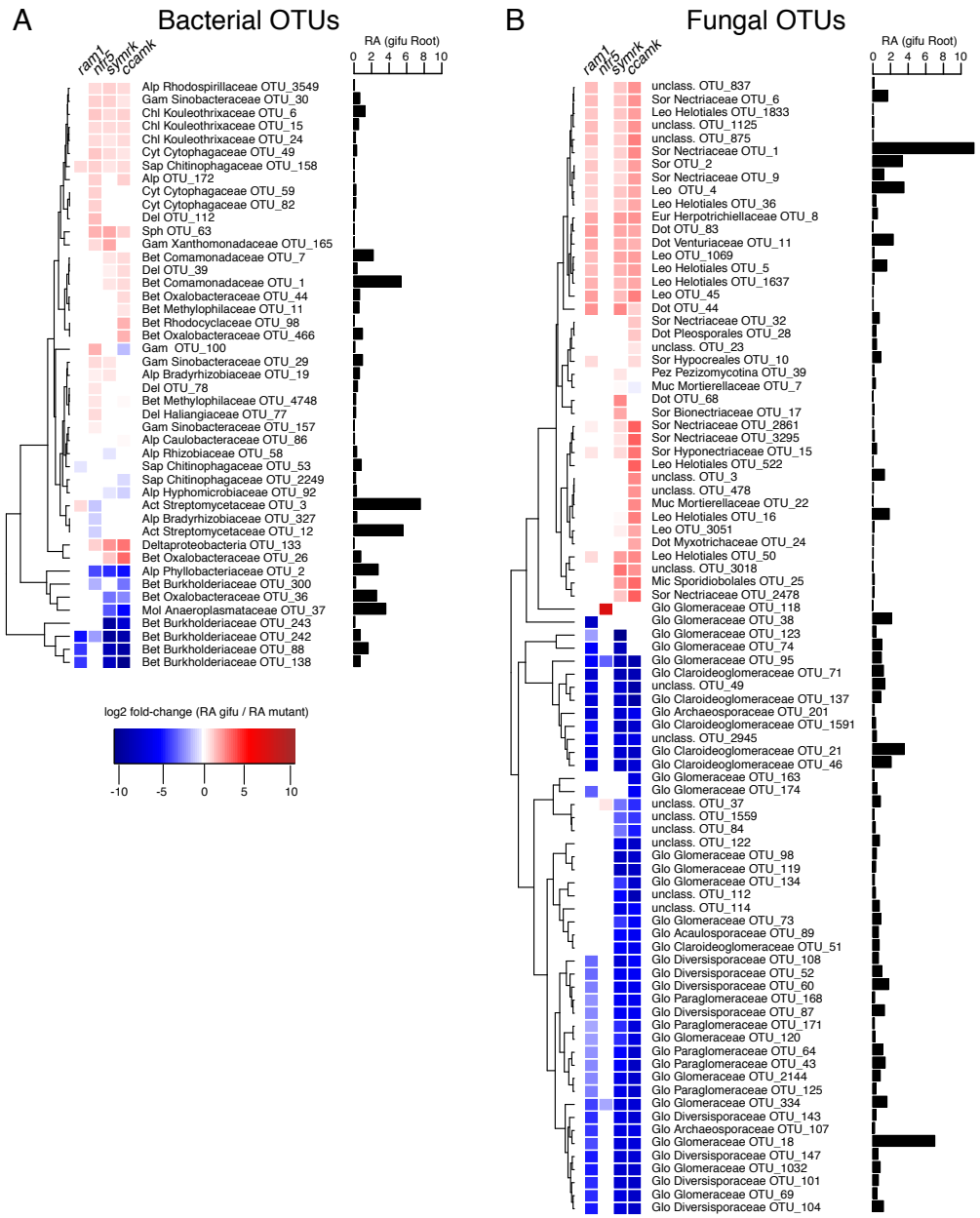

Fig5, **Differential abundance analysis for root associated OTUs**.
A) Bacterial OTUs that are differentially abundant in the roots of mutants compared to wt roots. B) fungal OTUs that are differentially abundant in the roots of mutants compared to wt roots. Only OTUs that have an average RA > 0.1% across all root samples, including mutants, are considered here. For each OTU the fold change in RA from wt to mutant is indicated ($P < 0.05$, Kruskal-Wallis test). Next to each OTU the RA in wt roots is indicated. Phylum and family asscociation (if available) is given for each OTU (Bacterial phyla: Del=Deltaproteobactria, Gem=Gemm-1 , Chl=Chloroflexi, Bet=Betaproteobacteria, Alp=Alphaproteobacteria, Gam=Gammaproteobacteria, Cyt=Cytophagia, Sap=Saprospirae, Ped=Pedosphaerae, Sph= Sphingobacteria, Mol= Mollicutes ; Fungal phyla: Sor=Sordariomyctes, Dot=Dothideomycetes, Mic= Microbotryomycetes, Ust=Ustilaginomycetes, Eur=eurotiomycetes, Leo=Leotiomycetes, Aga=Agaricomycetes, Glo=Glomeromyctes, Pez=Pezizomycota, Muc=Mucoromycotina).

Supplementary Figures

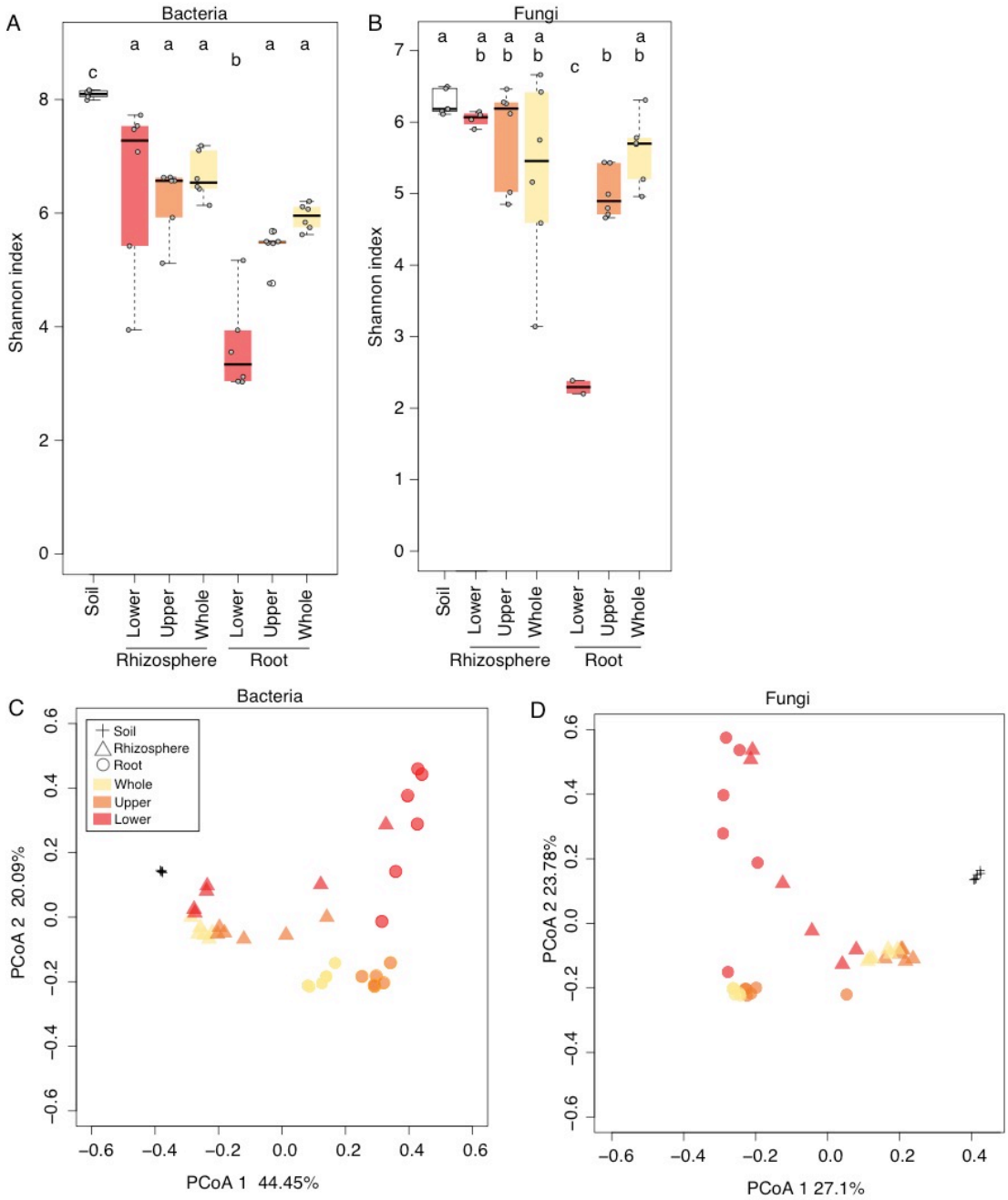

Supp Fig1, Alpha and beta diversity across root fractions.
A) Shannon diversity index for 16S amplicon data, soil (n=6), lower (n=6), upper (n=6), whole root fractions (n=6), and respective rhizosphere samples (n=6 each) B) Shannon diversity index for ITS2 amplicon data, soil (n=6), lower (n=2), upper (n=6), whole root fractions (n=6), and respective rhizosphere samples (n=6 each, except lower, n=4) (ANOVA with Tukey's post hoc test, P<0.05). C) Principal coordinate analysis of Bray-Curtis distances for bacterial data. D) Principal coordinate analysis of Bray-Curtis distances for fungal data.

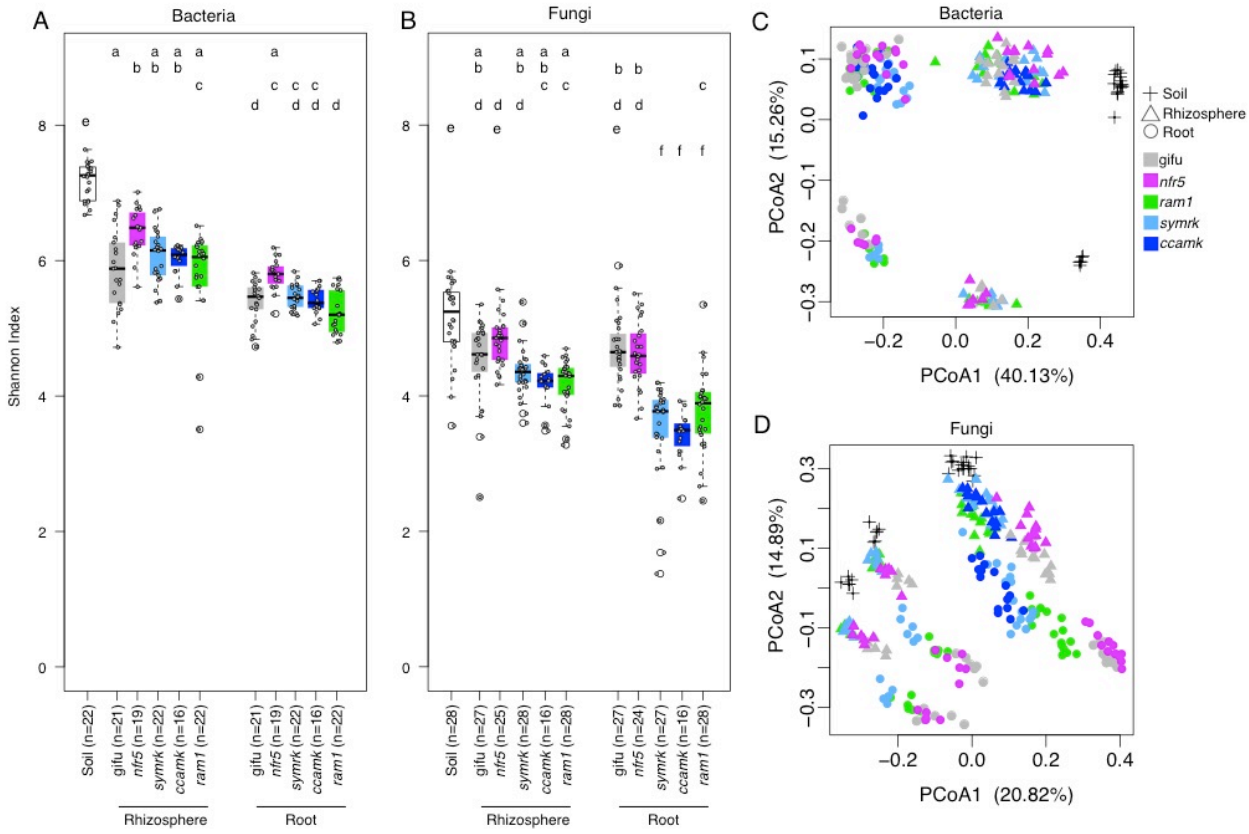

Supp Fig2, Alpha and beta diversity across plant compartments and genotypes.
A) Shannon diversity indices for the bacterial (16S amplicon) dataset. B) Shannon diversity indices for the fungal (ITS2 amplicon) dataset (ANOVA with Tukey's post hoc test, $P<0.05$) C) Principal coordinate analysis of Bray-Curtis distances for the bacterial dataset (n=222). D) Principal coordinate analysis of Bray-Curtis distances for the fungal dataset (n=274).

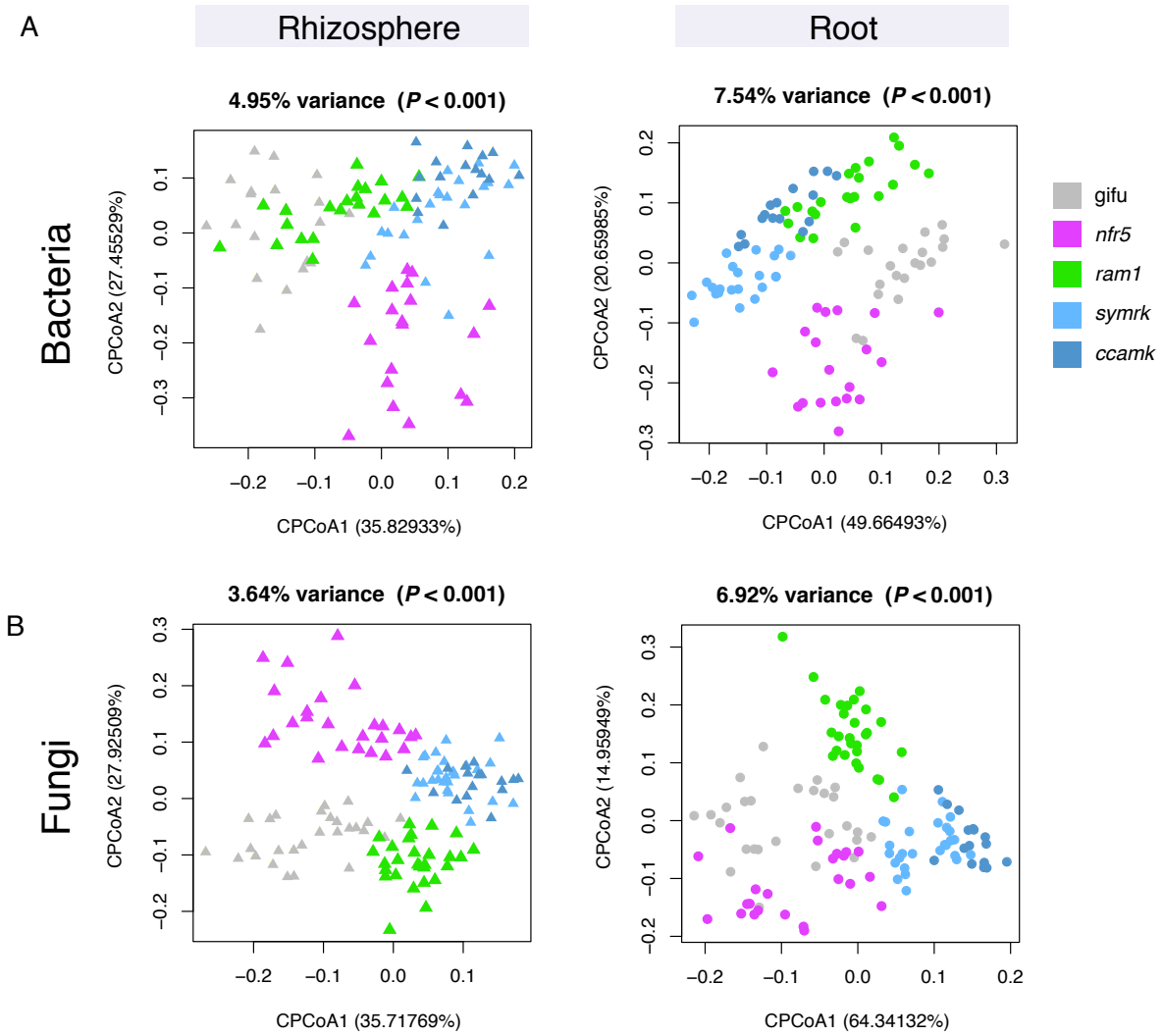

Supp Fig3, CPCoA, showing the same results as Fig3, but without known symbionts. Results are separated by compartments. Datasets were constrained by genotype, and filtered for effects of experiments and soil type. A) Bacterial dataset from which OTUs belonging to the Phyllobacteriaceae were removed before analysis (root n=100, rhizosphere n=100). B) Fungal dataset from which OTUs belonging to the Glomeromycota were removed before analysis (root n=122, rhizosphere n=124).

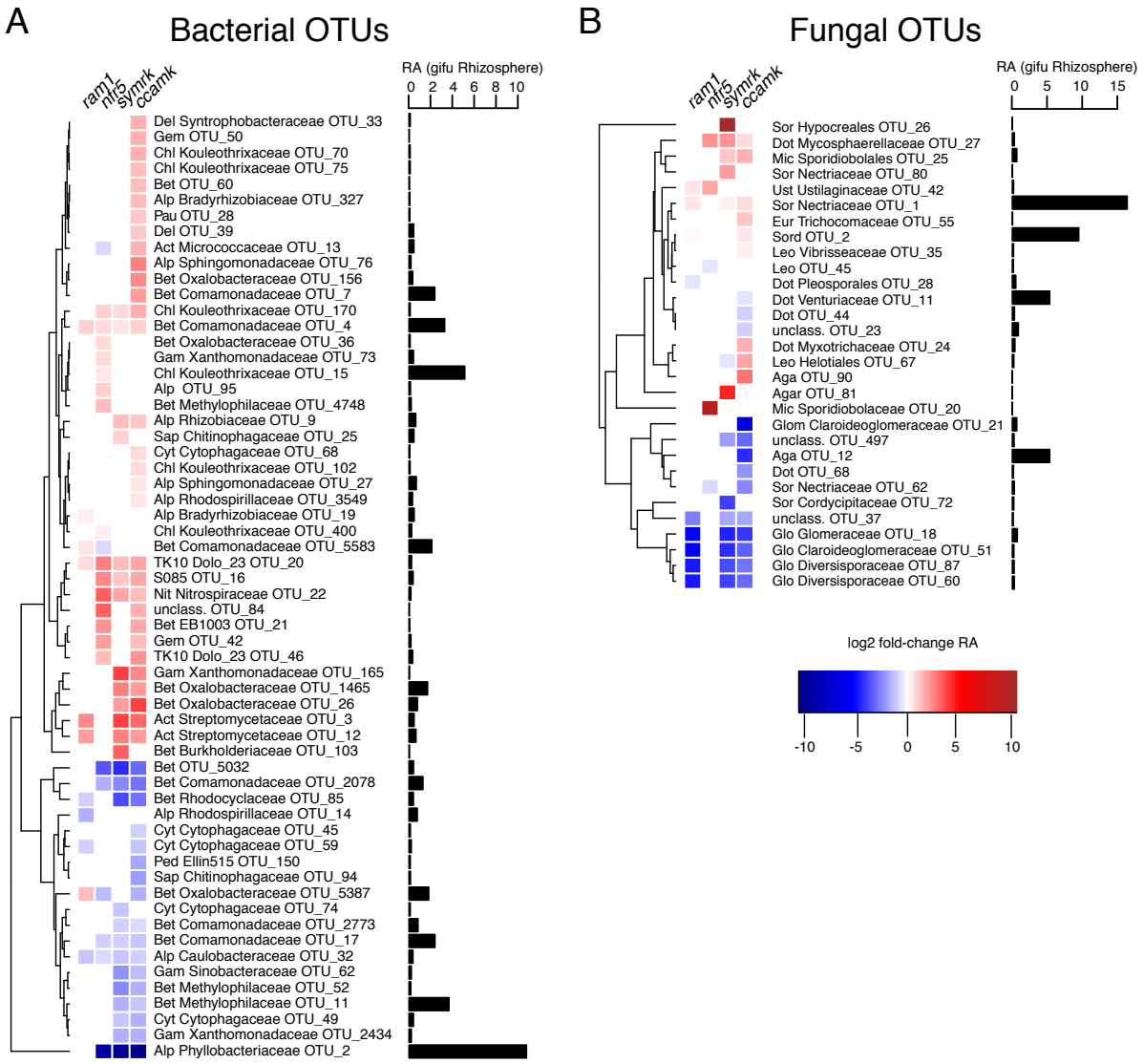

Supp Fig4, Differential abundance analysis for rhizosphere-associated OTUs showing enrichment and depletion in mutants.

A) bacterial OTUs that are differentially abundant in the rhizosphere of mutants compared to wt. B) fungal OTUs that are differentially abundant in the rhizosphere of mutants compared to wt. Only OTUs that have an average RA > 0.1% across all rhizosphere samples, including mutants, are considered here. For each OTU, the fold change in RA from wt to mutant is indicated ($P < 0.05$, Kruskal-Wallis test). Next to each OTU the RA in wt rhizosphere is indicated. Phylum and family asscociation is given for each OTU (Bacterial phyla: Del=Deltaproteobacteria, Gem=Gemm-1 , Chl=Chloroflexi, Bet=Betaproteobacteria, Alp=Alphaproteobacteria, Gam=Gammaproteobacteria, Cyt=Cytophagia, Sap=Saprospirae, Ped=Pedosphaerae, Sph= Sphingobacteria, Mol= Mollicutes ; Fungal phyla: Sor=Sordariomyctes, Dot=Dothideomycetes, Mic= Microbotryomycetes, Ust=Ustilaginomycetes, Eur=Eurotiomycetes, Leo=Leotiomycetes, Aga=Agaricomycetes, Glo=Glomeromyctes, Pez=Pezizomycota, Muc=Mucoromycotina).

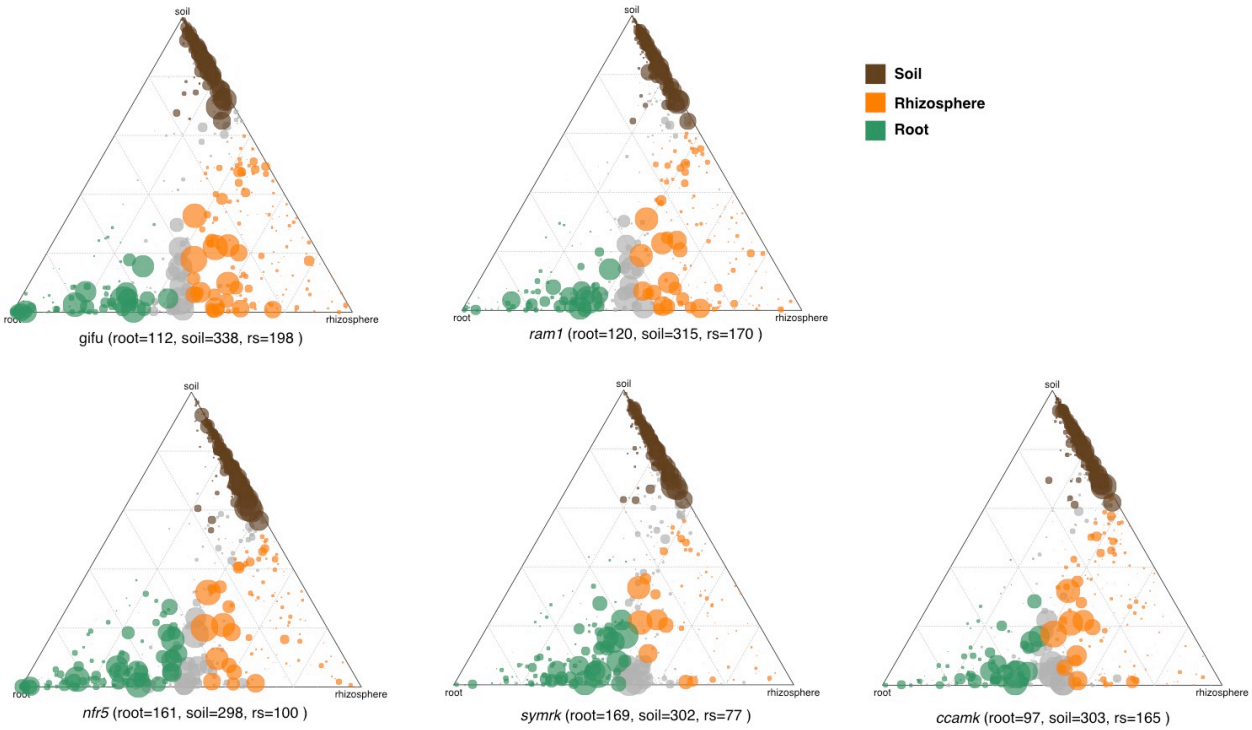

Supp fig5, Ternary plots showing compartment-enriched bacterial OTUs. Separately for wt and mutant plants. Below each plot the number of enriched OTUs for each compartment is shown.

787
788 **Supp table1, Symbiotic phenotype of *Lotus japonicus* wild-type and mutants grown in Cologne**
789 **soil** (*n=5*)
790

Genotype	WT(Gifu)	*nfr5-2*	*ram1-2*	*symrk-2*	*ccamk-13*
Colonization (% of root system with intraradical colonisation)	60-70	60-70	10	0	0
Arbuscules	present	present	present	none	none
Nodulation (% of roots with nodules)	100	0	100	0	0

791